Plasmon resonance induced photoconductivity of $ZrO_2(Y)$ films with embedded Au nanoparticles

D A Liskin[1], D O Filatov[2], O N Gorshkov[2], A P Gorshkov[1,2], I N Antonov[2], M E Shenina[2], S Y Zubkov[2] and D S Sinutkin[1]

[1] Department of Physics, Lobachevsky State University of Nizhny Novgorod, Nizhny Novgorod 603950, Russia
[2] Research and Educational Center for Physics of Solid State Nanostructures, Lobachevsky State University of Nizhny Novgorod, Nizhny Novgorod 603950, Russia

Email: dmitry_liskin@mail.ru

Abstract. We report on the experimental observation of photoconductivity (PC) in ultrathin (≈ 40 nm thick) $ZrO_2(Y)$ films with single layered arrays of Au nanoparticles (NPs) of 1 to 3 nm in diameter. The samples were prepared by the deposition of islanded Au films of ~1 nm in thickness sandwiched between two $ZrO_2(Y)$ layers by Magnetron Sputtering followed by annealing. The effect of PC was attributed to the photoexcitation of the collective plasmon oscillations in dense Au NP arrays. The temperature dependencies and kinetics of PC have been studied. At 300 K, the PC has been found to originate mainly from heating of $ZrO_2(Y)$ due to plasmon optical absorption in Au NPs (the bolometric effect). At 77 K, the photoresponse has been attributed to plasmon-assisted electron transport between NPs via the vacancy α-band in $ZrO_2(Y)$ barriers.

1. Introduction

The investigations of photoconductivity (PC) of the nanocomposite materials with the metallic nanoparticle (MNP) arrays embedded into the dielectric matrices due to the optically excited collective plasmonic oscillations in the MNPs have attracted an increasing interest in recent years [1]. The effect of PC in such systems is considered to be promising for various applications in novel integrated optics and photonic devices, such as photodetectors, optical switches, etc. [2]. There were many publications devoted to the investigations of collective plasmon excitations in MNP arrays [3]. However, the details of the PC mechanisms in the dielectric films with embedded MNPs, namely how the energy of the plasmon oscillations in the MNPs is converted into the change of the electrical conductivity of the nanocomposite films is not clear yet. Several models of the PC mechanism have been proposed in the literature. Thus, in [4] the PC in two-dimensional (2D) arrays of closely-packed Au nanoparticles (NPs) of 2 to 3 nm in diameter in the alkane-thiol films prepared on the SiO_2/Si substrates by the Langmuir-Blodgett technique has been studied. A pronounced peak at the plasmon resonance (PR) wavelength $\lambda_p \approx 600$ nm in the MNP array has been observed in the PC spectrum. Therefore, the authors concluded the PC to originate from the excitation of the surface plasmon-polariton oscillations in MNP arrays [5]. The effect was attributed to the increasing of the conductivity of the alkane matrix due to heating because of the plasmonic optical absorption in MNPs, i. e. the PC had a bolometric

nature. In [6], the PC in 2D Ag NP arrays in a porous Al_2O_3 film was investigated. The PC was attributed to the electron tunneling between MNPs across thin (~ 1 to 10 nm) Al_2O_3 barriers stimulated by surface plasmon-polaritons in Ag NPs. In [7], the collective plasmon excitation induced PC in Au NP arrays dispersed in the porphyrin (dithiol-PZn_3) has been studied. In that case, the dielectric matrix was able to manifest the PC itself, and the role of Au NPs was limited to the enhancement of the light energy concentration between MNPs due to collective plasmon oscillations. This, in turn, enhanced the PC in the porphyrin-filled gaps between Au NPs.

Summing up the above, one can conclude the PC mechanism in the nanocomposite films to depend strongly on the properties of the dielectric matrix. In the present study, the PC in ultrathin yttria stabilized zirconia ZrO_2(Y) films with embedded Au NP arrays (ZrO_2(Y):NP-Au films) has been investigated. It is worth noting that the PC in transition metal oxides with embedded MNPs has not been studied to date. An important distinctive feature of ZrO_2 is that the oxygen vacancies generate the deep donor states in the energy gap of this material with the energy E_c – 0.3 eV where E_c is the conduction band edge [8]. In ZrO_2(Y) with the cubic elementary cell, the oxygen vacancy is a crystal structure element, and the vacancy concentration is defined by the one of Y atoms [8]. When the Y molar fraction is ≥ 0.1, the oxygen vacancy related donor levels create a defect band (α-band), and the electron transport in this band plays an important role in the electron conductivity mechanism in ZrO_2(Y).

The goal of the present work was to study the mechanisms of the collective plasmon excitation inducted PC in the interacting Au NP arrays embedded into thin ZrO_2(Y) films.

2. Experimental details

The ZrO_2(Y) films were deposited by high frequency (HF) Magnetron Sputtering in Ar-O_2 gas mixture environment (50:50 % mol.) at the pressure of ~10^{-2} Torr from the powder oxide targets using a Torr International® MSS-3GS vacuum system for thin film deposition. The molar fraction of the stabilizing oxide Y_2O_3 in the target material was ≈ 0.12. The substrate temperature was T_g ≈ 300 °C.

The nanocomposite ZrO_2(Y)-based films were deposited onto the fused silica substrates polished to the optical quality. For the PC measurements, the Au(20 nm)/Cr(20 nm) strip-wise electrodes with the width of ~ 1 mm with the butterfly-wise gaps were formed on the substrate surface by standard optical photolithography prior to the deposition of the nanocomposit films. A schematic representation of the electrode configuration is presented in figure 1(a). The initial Au films with Cr sublayers were deposited by direct current (DC) Magnetron Sputtering in Ar ambient at T_g = 200 °C. The width of the gaps between the electrode tips was ~1 μm. Some areas on the substrate surface were left free of electrodes for the optical transmission spectra measurements. First, the underlying ZrO_2(Y) layers of ≈20 nm in thickness were deposited onto the silica glass substrates with the Au/Cr electrodes. Then, the islanded Au films with the nominal thickness d_{Au} = 0.5 to 2.0 nm were deposited by dc Magnetron Spattering at T_g = 200 °C.

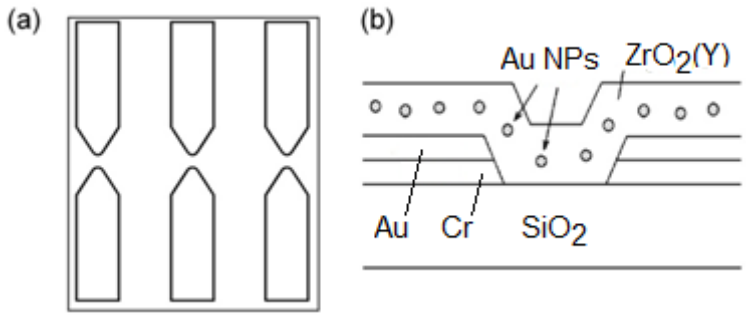

Figure 1. Schematic representation of a ZrO_2(Y):NP-Au/SiO_2 sample for PC measurements. (a) electrode configuration (top view); (b) **a** cross-section along a strip electrode axis.

In turn, the islanded Au films were capped by the ≈ 20 nm thick cladding ZrO_2(Y) layers deposited in the same conditions as the underlying one. Finally, the samples were annealed in Ar ambient at 450°C during 1 hour. The resulting structure of the nanocomposite film in the gap between the tips of the Au/Cr electrodes is shown schematically in figure 1(b). Earlier, High Resolution Cross-sectional Transmission Electron Microscopy (HR X-TEM) studies have shown the islanded Au films in the ZrO_2(Y)/Au/ZrO_2(Y) stacks prepared as described above to coagulate into Au NPs during annealing under certain conditions [9]. The nearly spherical Au NPs with a diameter, *D,* of 1 to 3 nm were arranged almost in a single sheet inside ZrO_2(Y) films. The average spacing between Au NPs in the 2D arrays, ℓ, was found to be from 3 to 4 nm, and the density parameter of the arrays $a = D/\ell$ was from 0.3 to 0.6.

Along with the ZrO_2(Y)-based samples, the samples based on ZrO_2 and GeO_2 films with Au NPs formed under the same conditions have been fabricated. GeO_2 is featured by dominating covalent-type chemical bonding, different crystal structure, and the electronic properties of the structural defects as compared to ZrO_2(Y). Particularly, there is no α-band in ZrO_2 as well as in GeO_2. Besides, the oxygen ion mobility in GeO_2 is much lower than the one in ZrO_2(Y). A comparative study of the PC in the samples based on different materials was expected to help clarifying the details of the PC mechanism in ZrO_2(Y), particularly, the role of the α-band in this one. Also, the pure films from the above materials of ≈ 40 nm in thickness without MNPs as were fabricated to serve as the reference.

The optical transmission spectra of the nanocomposite films were measured at 300 K using a Varian® Cary™ 6000i spectrophotometer. More details on the technique and the results of the optical transmission spectroscopy of the nanocomposite films similar to the ones investigated in the present work can be found in [9].

The PC measurements were carried out by the standard lock-on technique. A number of continuous wave semiconductor laser diodes (LDs) with the emission wavelengths λ ranging from 405 nm to 660 nm were applied as monochromatic photoexcitation sources. The LD emission was focused onto the gaps in the strip-wise electrodes on the sample surfaces in the spots of ~1 mm in size. The LD beam was chopped by a Stanford Research® SR-540 chopper with a frequency, *f,* of 6 to 350 Hz. The LD emission power was up to 1.5 W and was attenuated by a set of the neutral (grey) light filters. The bias voltage V_b = 10 V was applied to the electrodes, and the samples were loaded onto the current input of a Stanford Research® SR-810 digital lock-on detector. The dark current at V_b = 10 V measured with an Agilent® B1500A semiconductor device analyzer was ≈ 0.5 pA. To measure the temperature dependencies of the PC and of the dark current, the samples were immersed into a glass Dewar flask filled with liquid nitrogen.

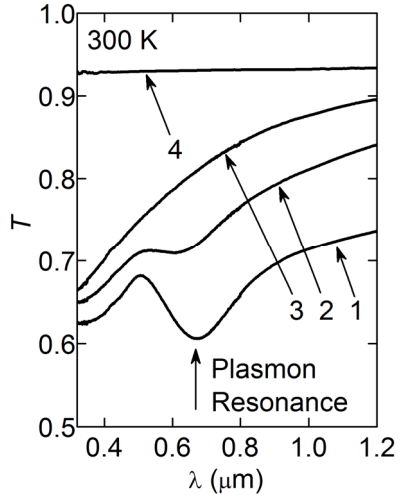

Figure 2. Optical transmission spectra of ZrO_2(Y):NP-Au/SiO_2 films. Initial Au nominal thickness d_{Au}, nm: *1* — 2.0; *2* — 1.0; *3* — 0.5. *4* — reference (SiO_2 substrate).

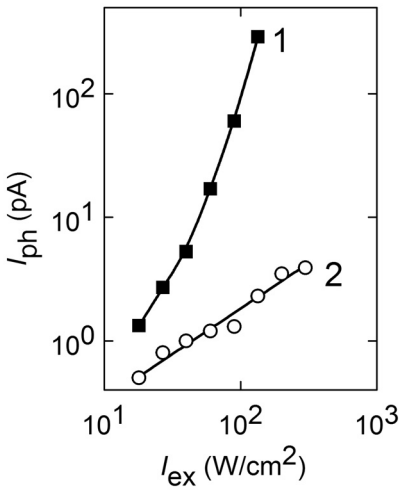

Figure 3. Dependence of PC in ZrO_2(Y):NP-Au film (d_{Au} = 2.0 nm) on the photoexcitation intensity I_{ex} at λ = 660 nm. *T*, K: *1* – 300; *2* – 77.

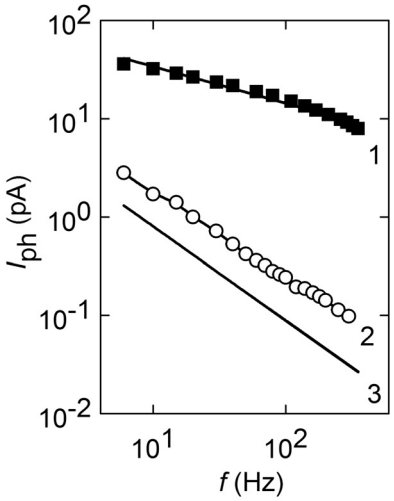

Figure 4. Dependence of PC in ZrO_2(Y):NP-Au films (d_{Au} = 2.0 nm) on the chopper frequency *f* (300 K): *1, 2* – experiment; *3* – calculation. I_{ex} = 65 W/cm^2, λ = 660 nm. Y molar fraction: *1* – 0.12, *2* – 0.

3. Results and discussion

Figure 2 shows the optical transmission spectra of the ZrO_2(Y):NP-Au films with different values of d_{Au}. A well expressed plasmon absorption peak was observed at λ ≈ 680 nm for d_{Au} = 2.0 nm (figure 2, curve 1). The intensity of the plasmon absorption peak decreased with decreasing d_{Au} (figure 2, curves 2 and 3). It is worth noting that the PR wavelength calculated for the individual Au NPs with the sizes specified above in the ZrO_2(Y) matrix according to the Mie scattering theory [10], λ_p = 590 to 600 nm. The red shift of the PR observed in the experiment relative to the calculated values of λ_p for the non-interacting NPs was attributed to the collectivization of plasmon excitations in dense Au NP arrays.

The values of photocurrent I_{ph} measured in ZrO_2(Y): NP-Au films were within the range of 1 to 100 pA that was well above the dark current as well as the noise level (~ 0.1 pA). The PC depended on the photoexcitation intensity I_{ex} superlinearly at 300 K (figure 3). On the other hand, we haven't observed any PC above the noise level in the reference ZrO_2(Y) films without Au NPs. All the above allowed us to attribute the PC in ZrO_2(Y): NP-Au films to the plasmon excitations in Au NPs.

The PC at λ = 660 nm (300 K) decreased with increasing chopping frequency *f* (figure 4, curve 1). Such a behavior is typical for the case when PC is measured by the lock-on technique, and $f^{-1} << \tau$ where τ is the PC decay time. Assuming the exponential PC decay law, the relation between the steady state PC I_0 (at $f \to 0$) and the amplitude of the 1st harmonic of the PC I_{ph} registered by the lock on detector is given by the following formula [11]:

$$I_{ph} = I_0 \mathrm{th}\left(\frac{1}{4f\tau}\right) \quad (1)$$

The decay time τ > 1 s could originate from the stray capacitance of the measurement circuit, *C*, which was ~10 pF. Indeed, for I_{ph} ~ 10 pA at V_b = 10 V one has the effective sample resistance $R = V_b/I_{ph} \sim 10^{12}$ Ω that gives *RC* ~ 10 s. However, at 77 K the PC didn't depend on *f*. To explain the frequency dependence of PC, we suggested the PC to originate from heating of the film material due to the plasmonic light absorption in NPs [12], i. e., the PC of ZrO_2(Y):NP-Au films had a bolometric nature as in [5]. In order to confirm this hypothesis, we have solved the time-dependent one-dimensional heat

transfer equation. The NP layer was considered as a δ-type heat source. The relation between the time dependent temperature and resistance of the ZrO_2(Y):NP-Au film was extracted from the results of the dark current temperature dependence measurements. The model $I_{ph}(f)$ dependence is presented in figure 4 (curve 3). One can see a qualitative agreement between the model $I_{ph}(f)$ dependence and the measured one. Within the framework of the bolometric mechanism, the independence of PC on f at 77 K was explained by a negligible dark current because it was found to obey the Mott law that, in turn, is typical for the hopping conductivity via the α-band in ZrO_2(Y) [8]. However, one can see in figure 4 that heating is not enough to explain the PC magnitude observed in the experiment. Moreover, the slope of the model $I_{ph}(f)$ dependence (figure 4, curve 3) is greater than the one of the dependence measured experimentally (figure 4, curve 1). In addition, the $I_{ph}(I_{ex})$ dependence at 77 K in figure 3 is sublinear (the power index was ≈ 0.73) while the one measured at 300 K is essentially superlinear. The latter agrees with the proposed bolometric mechanism as the heat transfer rate, in general, increases with increasing heat generation intensity in Au NPs. Nevertheless, all the observations presented above point to different PC mechanisms at various temperatures. So far, other PC mechanisms should be considered along with the bolometric one.

Potentially, the PC in ZrO_2(Y):NP-Au films could be attributed to the internal photoemission of the electrons from the Fermi level in Au NPs into the conduction band of ZrO_2(Y). However, the potential barrier height at the Au/ZrO_2(Y) interface is ≈ 2.4 ± 0.1 eV at 300 K [13] (see the calculated band diagram of Au NPs in the ZrO_2(Y) matrix in figure 5). At the same time, the photon energy hv corresponding to λ = 660 nm is ≈ 1.9 eV that is not enough for the internal photoemission.

On the other hand, hv ≈ 1.9 eV is almost enough to excite the electrons from the Fermi level in Au NPs into the α-band in ZrO_2(Y) barriers. The excitation of electron into the α-band can also be associated with the electron tunneling through the triangle barrier at the Au/ZrO_2(Y) interface, as shown schematically in figure 5. Taking into account the PR in Au NPs to occur during the illumination with λ = 660 nm, one can expect the mechanism of the optical excitation of the electrons from Au NPs into the α-band in ZrO_2(Y) barriers in the conditions of the plasmon resonance in Au NPs to be an efficient one [6].

It should be stressed here that we haven't observed any PC signal in ZrO_2:NP-Au films above the noise level at 77 K that can be explained by the absence of the α-band in ZrO_2, in contrary to ZrO_2(Y). At 300 K, the observed values of PC in a ZrO_2:NP-Au film with d_{Au} ≈ 2.0 nm (figure 4, curve 2) were much closer to the expected values for the bolometric mechanism (figure 4, curve 3) than the ones for the ZrO_2(Y):NP-Au film (figure 4, curve 1). In addition, the slope of the experimental dependence $I_{ph}(f)$ was close to the slope of the model one (cf. curves 2 and 3 in figure 4). All the above allowed us to conclude the PC observed in ZrO_2:NP-Au films to have a pure bolometric nature.

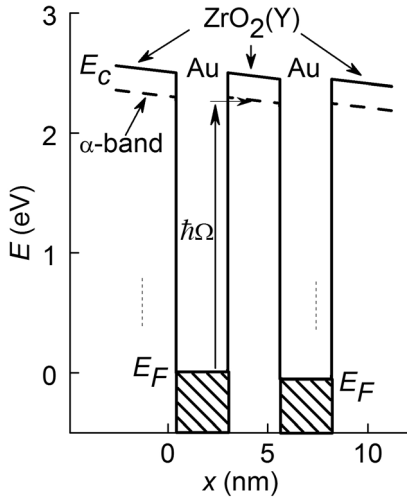

Figure 5. Calculated band diagram (300 K) of Au NPs in ZrO_2(Y) film in the external electric field applied between the Au/Cr electrodes (figure 1). D = 3 nm; V_b = 10 V; $\hbar\Omega$ is the collective plasmon-polariton energy in the Au NP array.

This fact, in turn, supports the proposed mechanism of PC in ZrO_2(Y):NP-Au films related to the plasmon-assisted excitation of the electrons from the Fermi level in Au NPs into the α-band in ZrO_2(Y) barriers and the electron transport to the adjacent Au NPs via the α-band.

We haven't observed any PC in GeO_2-based films (neither with nor without Au NPs). This fact can be explained by the following. The potential barrier height at the Au/GeO_2 interface can be estimated as ≈ 3.5 eV according to [14] whereas the PR in the optical transmission spectra of the GeO_2:NP-Au film has been observed at $h\nu \approx 2.3$ eV (for $d_{Au} \approx 2.0$ nm) that is surely not enough for the plasmon-assisted tunneling between NPs.

4. Conclusion

The results of the present study have demonstrated the nanocomposite ZrO_2(Y) films with embedded single sheet arrays of Au NPs to exhibit the PC under excitation at the wavelength corresponding to the plasmon optical absorption resonance. The effect was attributed to the optical excitation of the collective plasmonic oscillations in the dense Au NP arrays. The investigations of the PC kinetics have revealed two components of the photoresponse dominating at different temperatures. The slow component related to the bolometric effect due to heating of the ZrO_2(Y) matrix between NPs because of the plasmon optical absorption in Au NPs predominates at 300 K. The bolometric effect is absent at 77 K, when the fast component related to the plasmon-assisted excitation of electrons into the oxygen vacancy related α-band in ZrO_2(Y) barriers and the electron transport to the adjacent NPs via the α-band dominates.

Thus it was established that the nanocomposite ZrO_2(Y) films with embedded single sheet arrays of Au NPs demonstrate the PC under the excitation wavelength corresponds to the plasmon optical absorption resonance. The effect is attributed to the optical excitation of the collective plasmonic oscillations in the dense Au NP arrays.

Acknowledgments

The authors gratefully acknowledge the financial support from Ministry of Education and Science of the Russian Federation (Project # 3.2441.2014/K).

References

[1] Hwang J D, Wang F H, Kung C Y, Lai M J and Chan M C 2014 *J. Appl. Phys.* **115** 173110
[2] Atwater H A and Polman A 2010 *Nature Mater.* **9** 205
[3] Pelton M, Aizpurua J and Bryant G 2008 *Laser & Photon.* **2** 136
[4] Hashimoto T, Fukunishi Y, Zheng B, Uraoka Y, Hosoi T, Shimura T and Watanabe H. *Appl. Phys. Lett*. **102** 083702
[5] Mangold M A, Weiss C, Calame M and Holleitner A. W 2009 *Appl. Phys. Lett*. **94** 161104
[6] Huang C-H, Lin H-Y, Lau B-C, Liu C-Y, Chui H-C and Tzeng Y 2010 *Opt. Express*. **18** 27891
[7] Banerjee P, Conklin D, Nanayakkara S, Park T-H, Therien M J, Bonnell D A 2010 *ACS Nano*. **4** 1019
[8] Abbas H A 2012 *Stabilized Zirconia for Solid Oxide Fuel Cells or Oxygen Sensors. Characterization of Structural and Electrical Properties of Zirconia Doped with Some Oxides* (New York: LAP Lambert Academic)
[9] Gorshkov O N, Antonov I N, Filatov D O, Shenina M E, Kasatkin A P, Pavlov D A, Bobrov A I 2016 *Tech. Phys. Lett*. **42** 36
[10] Mie G 1908 *Ann. Phys*. **3**, 377
[11] Ryvkin S M 1950 *Sov. Phys. JETP* **20** 139
[12] Baffou G, Quidant R and Garcia de Abajo F J 2010 *Nano Lett*. **4** 709
[13] Filatov D O, Guseinov D V, Antonov I N, Kasatkin A P and Gorshkov O N 2014 *RSC Advances* **4** 57337
[14] Shaposhnikov A V, Perevalov T V, Gritsenko V A, Cheng C H and Chin A 2012 *Appl. Phys. Lett*. **100** 243506